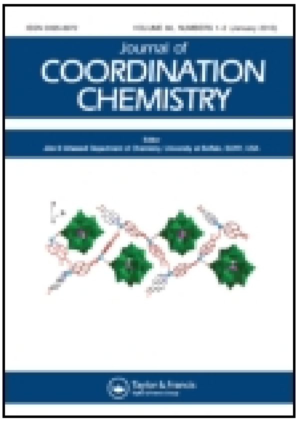

Journal of Coordination Chemistry
Publication details, including instructions for authors and subscription information:
http://www.tandfonline.com/loi/gcoo20

Preparation, configurational and DFT-NBO analysis of nickel(II) complexes with edta-type ligands containing six-membered backbone ring: crystal structure of $[Ni(H_2O)_6][Ni(1,3\text{-pdta})]\cdot 2H_2O$

Svetlana Belošević [a], Miorad M. Vasojević [a], Marija S. Jeremić [a], Auke Meetsma [b] & Zoran D. Matović [a]

[a] Faculty of Science, Department of Chemistry, University of Kragujevac, Kragujevac, Serbia

[b] Stratingh Institute for Chemistry and Chemical Engineering, University of Groningen, Groningen, The Netherlands

To cite this article: Svetlana Belošević, Miorad M. Vasojević, Marija S. Jeremić, Auke Meetsma & Zoran D. Matović (2013) Preparation, configurational and DFT-NBO analysis of nickel(II) complexes with edta-type ligands containing six-membered backbone ring: crystal structure of $[Ni(H_2O)_6][Ni(1,3\text{-pdta})]\cdot 2H_2O$, Journal of Coordination Chemistry, 66:10, 1730-1745, DOI: 10.1080/00958972.2013.789104

To link to this article: http://dx.doi.org/10.1080/00958972.2013.789104

Journal of Coordination Chemistry, 2013
Vol. 66, No. 10, 1730–1745, http://dx.doi.org/10.1080/00958972.2013.789104

Preparation, configurational and DFT–NBO analysis of nickel(II) complexes with edta-type ligands containing six-membered backbone ring: crystal structure of $[Ni(H_2O)_6][Ni(1,3\text{-pdta})]\cdot 2H_2O$

SVETLANA BELOŠEVIĆ†, MIORAD M. VASOJEVIĆ†, MARIJA S. JEREMIĆ†,
AUKE MEETSMA‡ and ZORAN D. MATOVIĆ*†

†Faculty of Science, Department of Chemistry, University of Kragujevac, Kragujevac, Serbia
‡Stratingh Institute for Chemistry and Chemical Engineering, University of Groningen, Groningen, The Netherlands

(*Received 16 October 2012; in final form 23 January 2013*)

New hexadentate nickel(II) complex $Mg[Ni(1,3\text{-pd3ap})]\cdot 10H_2O$ containing unsymmetrical edta-type ligand, 1,3-propanediamine-*N,N,N′*-triacetate-*N′*-3-propionate (1,3-pd3ap), has been prepared, chromatographically separated, and characterized. Only one [*trans*(O_5)] of the two possible geometrical isomers was isolated. In this isomer, the two five-membered glycinate rings (R rings) occupy *trans*-axial sites while the one glycinate ring and one *β*-alaninate ring lie in the equatorial plane with the two diamine nitrogens (G rings). This result confirms the assignment made on the basis of the density functional theory (DFT), IR, and UV–Vis spectral data analysis. In order to see cation influence on the structural and electronic behavior, $[Ni(H_2O)_6][Ni(1,3\text{-pdta})]\cdot 2H_2O$ complex has also been prepared and its structure verified by an X-ray analysis. Spectral data and electronic transition assignment, DFT–natural bonding orbital, and an extensive strain analysis are discussed in comparison with those of other $[Ni(\text{edta-type})]^{2-}$ complexes of known configuration.

Keywords: Preparation; Nickel(II) complexes; Crystal structure; Density functional theory; NBO

1. Introduction

Metals such as nickel, lead, cadmium, mercury, thallium manganese, chromium, and platinum are toxic, of major concern to the environment and human health. The effects of chelating agents and drugs used clinically as antidotes to metal toxicity were reviewed in several articles [1]. Nickel is considered as an essential element for all forms of life, occupying the active site of six diverse microbial enzymes: superoxide dismutase, urease, hydrogenase, methyl-CoM reductase, carbon monoxide dehydrogenase, and acetyl-CoA synthase [2], but there has been much more concern about the toxicity of Ni than about Ni deficiency. Food, drinking water, and contaminated air, including tobacco smoke and skin contact with metals containing nickel, are the main sources of exposure. Dietary intake of nickel greatly varies, depending on dietary habits, since certain types of food, such as cocoa,

---

*Corresponding author. Email: zmatovic@kg.ac.rs soybeans, some legumes, oatmeal, and various nuts, contain high nickel concentrations. Allergic dermatitis is the most common form of nickel toxicity in humans. Long-term exposure to nickel can result in chronic bronchitis and reduced lung function, as well as increased incidence of cancers of the lung and paranasal sinuses [3]. Damage to the liver, kidneys, adrenal glands, spleen, and brain is also possible. Our group continues research of M(III) and M(II) (particularly paying attention to Cu(II) and Ni(II)) complexes of edta-type diaminopolycarboxylate ligands in a decade long tradition [4–9].

Bonding angles exhibited by edta complexes (edta = ethylenediaminetetraacetate ion) are strained as shown by significant deviations from ideal values. The ethylenediamine ring (E ring) and the two glycinate rings (G rings) occupying an equatorial plane are more strained than the two glycinate rings coordinated axially (R rings) for $[M(edta)]^{n-}$ complexes (M = Co(III) [10], Cr(III) [11], Fe(III) [12], Mn(III) [13], Zn(II) [14], Cu(II) [14], Co(II) [15], and Ni(II) [16]). Moreover, the G rings are usually observed to be puckered, while the R rings are more planar, and are referred to as having an *envelope* conformation. The edta-like ligands with longer (diamine or carboxylate) chains are likely to function as hexadentate with metal ions of different size. Such ligands have less in-plane strain, thus allowing the complexes to attain octahedral angles closer to the ideal with apparently less strain in the M–L bonds by forming (as dominant) less-strained isomers. Generally, the molecular structures of edta and related transition-metal complexes have been discussed in terms of the d-electron configuration and size of the metal ion (M) and the structure of the ligand. These influence the differences in the bond lengths (M–N and M–O), ring strain, and the ligand configuration [5].

For ligands having mixed five- and six-membered carboxylate arms, geometrical isomers differ in the number (0, 1, 2) of six-membered rings lying in the equatorial plane (G plane). This group includes the following ligands: eda3p (eda3p = ethylenediamine-*N*-acetate-*N,N′,N′*-tri-3-propionate ion); ed3ap (ed3ap = ethylenediamine-*N,N,N′*-triacetate-*N′*-3-propionate ion); 1,3-pd3ap (1,3-pd3ap = 1,3-propanediamine-*N,N,N′*-triacetate-*N′*-3-propionate ion); *S,S*-edds (*S,S*-edds = 2*S*, 2*S′*-ethylenediamine-*N,N′*-disuccinate ion); eddadp (eddadp = ethylenediamine-*N,N′*-diacetate-*N,N′*-di-3-propionate ion); and 1,3-pddadp (1,3-pddadp = 1,3-propanediamine-*N,N′*-diacetate-*N,N′*-di-3-propionate ion).

Two symmetrical ligands (eddadp and 1,3-pddadp) can form three geometrical isomers upon coordination: *trans*(O_5), *trans*(O_5O_6), and *trans*(O_6) (figure 1). For $[Ni(eddadp)]^{2-}$, the favored isomer is *trans*(O_5)-$[Ni(eddadp)]^{2-}$ [6] because the six-membered 3-propionate chelating with a five-membered diamine serves better for the formation of less-strained G rings. Contrary to this, two of three possible isomers *trans*(O_5) and *trans*(O_5O_6) of $[Ni(1,3\text{-}pddadp)]^{2-}$ have been reported [7].

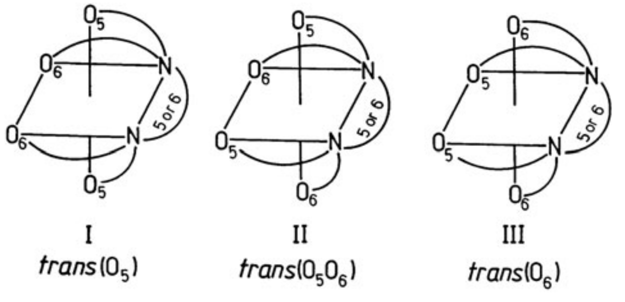

Figure 1. Geometrical isomerism of six-coordinate $[M(edta\text{-}type)]^{n-}$ complexes.

The unsymmetrical ed3ap with hexadentate coordination can yield two geometrical isomers differing in the position of the six-membered ring: *trans*(O_5) and *trans*(O_5O_6), but only one, the favored less-strained *trans*(O_5)-$[Ni(ed3ap)]^{2-}$ isomer, was prepared and separated [17]. For $[Ni(eda3p)]^{2-}$, two possible geometrical isomers are expected: *trans* (O_6) and *trans*(O_5O_6). The *trans*(O_5O_6)-$[Ni(eda3p)]^{2-}$ isomer is preferable in this case [17]. Structural data for closely related edta-like Ni(II) complexes are also known: $[Ni(1,3\text{-}pdta)]^{2-}$ [18] (1,3-pdta = 1,3-propanediaminetetraacetate ion); $[Ni(edtp)]^{2-}$ [6] [edtp = ethylenediaminetetra-3-propionate ion]; $[Ni(tdta)]^{2-}$ [19] (tdta = tetramethylenediaminetetraacetate ion); $[Ni(bdta)]^{2-}$ [20] (bdta = 1,4-butanediaminetetraacetate ion); $[Ni(1,3\text{-}pndta)]^{2-}$ [21] (1,3-pentanediaminetetraacetate ion).

In this article, we describe the syntheses of 1,3-propanediamine-*N,N,N′*-triacetic-*N′*-3-propionic acid and the preparation of corresponding nickel(II) complex along with coordination influence while changing cation from alkaline/alkaline-earth to transition metal. Therefore, we synthesized $[Ni(pdta)]^{2-}$ with corresponding Ni^{2+} cation, and X-ray data are reported for $[Ni(H_2O)_6]\cdot[Ni(1,3\text{-}pdta)]\cdot 2H_2O$. Structural parameters and strain analysis data of this complex and other similar complexes are compared and discussed in relation to the structure of the ligand, geometry of complexes, and their octahedral distortion. IR and electronic spectra of the investigated complexes are given here. In addition, molecular mechanics and density functional theory (DFT) methods have been used to model the most stable geometric isomer yielding significant structural data. The results from DFT studies have been compared with X-ray data. An extensive molecular orbital (natural bonding orbital (NBO)) and configuration analysis of the series of complexes is presented.

2. Experimental

2.1. *General*

All commercially available reagent-grade chemicals were used without purification. Barium(1,3-propanediamine-*N,N,N′*-triacetato-*N′*-3-propionato)cuprate(II)hexahydrate), $Ba[Cu(1,3\text{-}pd3ap)]\cdot 6H_2O$ was prepared according to unpublished procedure.

Elemental microanalyses for C, H, N were performed at the Microanalytical laboratory, Faculty of Chemistry, University of Belgrade, Serbia. IR spectra from 400 to 4000 cm^{-1} were recorded on a PerkinElmer FT-IR spectrophotometer Spectrum One using KBr pellets. Electronic absorption spectra were recorded on a PerkinElmer Lambda 35 spectrophotometer. For these measurements, 1×10^{-2} M aqueous solutions of the complexes under investigation were used. Melting points were measured by a Stuart melting device with accuracy ±1 °C.

2.2. *Preparation of 1,3-propanediamine-N,N,N′-triacetic-N′-3-propionic acid, (H_4 1,3-pd3ap)*

6.25 g (10 mmol) $Ba[Cu(1,3\text{-}pd3ap)]\cdot 6H_2O$ contains 1.37 g of barium (10 mmol), so we added 0.1 M H_2SO_4 to precipitate all the barium as $BaSO_4$. The deposited $BaSO_4$ was separated by filtration. The clear bright filtrate (pH∼1–2) was saturated with gaseous H_2S. The black suspension containing CuS was filtered and colorless filtrate concentrated to a small volume. pH of the clear solution was adjusted to 2–3 by adding 6 M HCl. Standing in refrigerator for several days, the turbid solid formed and was collected by vacuum filtration. Yield: 3.04 g (95%) of $H_4$1,3-pd3ap.

2.3. *Preparation of magnesium(1,3-propanediamine-N,N,N′-triacetato-N′-3- propionato) nickelate(II) decahydrate, Mg[Ni(1,3-pd3ap)]·10H$_2$O (1)*

The solution of NaOH (0.56 g, 14 mmol in 5 mL of water) (pH≈9) was added to 10 mL of solution containing 2.00 g (6.25 mmol) of $H_4$1,3-pd3ap. A solution of 1.48 g (6.25 mmol) $NiCl_2·6H_2O$ in 10 mL of water was added to that suspension (pH≈5), and blue solution was then heated (65 °C) for 1 h with stirring. The volume of the solution was maintained by periodic addition of hot water. The resulting solution was then desalted by passing it through a G-10 Sephadex column (2.5 × 40 cm) eluting with distilled water. The blue solution was poured into a 5 × 60 cm column containing Dowex 1-X8 (200–400 mesh) anion-exchange resins in Cl^- form. The column was then washed with water and eluted with 0.1 M $MgCl_2$. One band was obtained. The eluate was evaporated to 10 mL and desalted by passage through a G-10 Sephadex column, with distilled water as the eluent. After that the eluate was concentrated to 3 mL and stored in a desiccator over ethanol for several days. The blue powder was collected and air-dried. Yield: 0.80 g (22%) of Mg[Ni (1,3-pd3ap)]·10H_2O. Melting point: 218 °C. The elemental analysis is consistent with the composition of Mg[Ni(1,3-pd3ap)]·10H_2O; $C_{12}H_{36}N_2O_{18}MgNi$; Mw = 579.41. Found: C, 24.61; H, 6.12; N, 4.91 for the complex salt, Calcd: C, 24.87; H, 6.26; N, 4.83.

2.4. *Preparation of barium(1,3-propanediaminetetraacetate) dihydrate, Ba$_2$1,3-pdta·2H$_2$O*

The barium salt of 1,3-propanediaminetetraacetic acid was prepared according to the procedure of Weyh and Hamm [22], with a minor modification. The condensation mixture of 1,3-propanediamine (15 g, 0.20 mol) and chloroacetic acid (96 g, 0.91 mol) in aqueous KOH solution was prepared; deposited KCl was removed by filtration. A hot solution of $BaCl_2·2H_2O$ (98 g, 0.40 mol in 200 mL of H_2O) was then added to the mixture, which was stirred (90 °C) for 2 h. The white precipitate of $Ba_2$1,3-pdta·2H_2O, which was practically insoluble in water, was filtered, washed with warm water, and air-dried (≈100 g).

The elemental analysis is consistent with the composition of $Ba_2$1,3-pdta·2H_2O; $Ba_2C_{11}H_{18}N_2O_{10}$; Mw = 612.93. Found: C, 21.04; H, 2.63; N, 4.53; Ba, 44.74; H_2O, 5.90 for the Ba_2(1,3-pdta)·2H_2O, Calcd: C, 21.55; H, 2.96; N, 4.57; Ba, 44.81; H_2O, 5.88.

2.5. *Preparation of hexaaquanickel(II)-[(1,3-propanediaminetetraacetato)nickelate(II)] dihydrate, [Ni(H$_2$O)$_6$][Ni(1,3-pdta)]·2H$_2$O (2)*

$NiSO_4·7H_2O$ 8.43 g (30 mmol) was dissolved in 80 mL of water; the solution was stirred at 80 °C for 10 min. To this solution, solid Ba_2(1,3-pdta)·2H_2O 18.39 g (30 mmol) was added and the resulting light-blue solution was then stirred at 80 °C for 3 h. During this process, the volume of the reaction mixture was maintained by addition of hot water, and the pH of the mixture was kept at 7. After the deposited $BaSO_4$ was removed by filtration, the filtrate was reduced to 60 mL and then poured into a 5 × 60 cm column containing Dowex 1-X8 (200–400 mesh) anion-exchange resin in the Cl^- form. After the column was washed with H_2O, a 0.05 M $BaCl_2$ solution was used for elution (ca. 0.5 mL min^{-1}). One band with 2^- charge appeared on the column. The obtained eluate was reduced to 150 mL and then allowed to stand at room temperature for several days. The crystals of Ba[Ni(1,3-pdta)]·$8H_2O$ were collected. Ba[Ni(1,3-pdta)]·$8H_2O$ 1.28 g (2 mmol) was dissolved in a small amount of water. A solution of 0.56 g (2 mmol) $NiSO_4$·$7H_2O$ in a small amount of water was added to that suspension. The deposited $BaSO_4$ was removed by filtration. The filtrate was reduced to a small volume and then allowed to stand at room temperature for several days. Blue crystals were collected, washed with ethanol and then ether, and air-dried. Yield: 0.93 g (83%) of [Ni(H_2O)$_6$][Ni(1,3-pdta)]·$2H_2O$. Melting point: 181 °C. The elemental analysis is consistent with the composition [Ni(H_2O)$_6$][Ni(1,3-pdta)]·$2H_2O$; $C_{11}H_{30}N_2O_{16}Ni_2$; Mw = 563.75. Found: C, 23.70; H, 5.42; N, 5.01 for the complex salt, Calcd: C, 23.44; H, 5.36; N, 4.97.

2.6. *Crystal structure determination*

Suitable blue prism-shaped crystals were obtained by recrystallization from water. A crystal with dimensions of 0.51 × 0.31 × 0.25 mm was mounted on a glass fiber and aligned on a Bruker [23] SMART APEX CCD diffractometer (Platform with full three-circle goniometer). The crystal was cooled to 100(1) K and intensity measurements were performed using graphite monochromated Mo Kα radiation from a sealed ceramic diffraction tube (SIEMENS). The final unit cell was obtained from the *xyz* centroids of 9589 reflections after integration. Intensity data were corrected for Lorentz and polarization effects, scale variation, for decay and absorption: a multi-scan absorption correction was applied, based on the intensities of symmetry-related reflections measured at different angular settings (*SADABS*) [24] and reduced to F_o^2. The program suite *SHELXTL* was used for space group determination (*XPREP*) [23]. The unit cell [25] was identified as orthorhombic; reduced cell calculations did not indicate any higher metric lattice symmetry [26]. The space group *Pnna* was derived from the systematic extinctions. Examination of the final atomic coordinates of the structure did not yield extra crystallographic or metric symmetry elements [27,28]. The structure was solved by direct methods with SIR-97 [29]. The positional and anisotropic displacement parameters for the non-hydrogen atoms were refined. Final refinement on F^2 carried out by full-matrix least-squares techniques converged at $wR(F^2) = 0.0611$ for 2828 reflections and $R(F) = 0.0218$ for 2608 reflections with $F_o \geqslant 4.0\,\sigma(F_o)$ and 203 parameters and 0 restraints. The final difference Fourier map was essentially featureless: no significant peaks (0.44(9) e Å^{-3}) having chemical meaning above the general background were observed. The positional and anisotropic displacement parameters for the non-hydrogen atoms and isotropic displacement parameters for hydrogens were refined on F^2 with full-matrix least-squares procedures. All refinement calculations and graphics were performed with the program packages SHELXL [30] (least-square refinements), a locally modified version of the PLUTO [31] and PLATON [32] package (checking the final results for missed symmetry with the *MISSYM* option, solvent accessible voids with the *SOLV* option, calculation of geometric data and the ORTEP [32] illustrations). Crystal data, numerical details, and refinement are given in table 1.

2.7. *Computational method*

DFT calculations reported in this work were carried out using the Amsterdam density functional (ADF) 2007.01 [33–35] program package. This method was used to find the optimal

Table 1. Crystal data summary for $[Ni(H_2O)_6][Ni(1,3\text{-}pdta)]\cdot 2H_2O$.

Formula	$C_{11}H_{30}N_2O_{16}Ni_2$
Formula weight (g mol^{-1})	563.75
Crystal system	Orthorhombic
Space group, No.	*Pnna*, 52
a (Å)	13.2024(5)
b (Å)	11.6024(4)
c (Å)	13.6017(5)
V (Å^3)	2083.50(13)
Θ range unit cell: min.–max., deg; reflections	2.31–29.70; 9589
Z	4
ρ_{calc} (g cm^{-3})	1.797
F(0 0 0), electrons	1176
μ(Mo Kα) (cm^{-1})	18.9
Radiation type; λ (Å)	Mo Kα, 0.71073
Temperature (K)	100(1)
θ range; min. max. (°)	2.31, 29.70
Index ranges	h: −17→18; k: −12→15; l: −18→18
Total data, unique data	15,890, 2828
Data with criterion: ($F_o \geqslant 4.0\ \sigma\ (F_o)$)	2608
Number of reflections	2828
Number of refined parameters	203
$wR(F^2) = [[w(F_o^2 - F_c^2)2]/[w(F_o^2)^2]]^{1/2}$	0.0611
Weighting scheme: a, b	0.0347, 0.8508[a]
$R(F) = \Sigma(\lVert F_o\rvert - \lvert F_c\rVert)/\Sigma\lvert F_o\rvert$	0.0218
Difference Fourier map, e Å^{-3}	−0.51, 0.44(9)

[a] $w = 1/[\sigma^2(F_o^2) + (aP)^2 + bP]$ and $P = [\max(F_o^2, 0) + 2F_c^2]/3$.

geometries of octahedral Ni(II) complexes. Geometry optimization of all the investigated molecules was performed using the generalized gradient approximation (GGA) in the form given by Perdew–Wang (PW91) [36] characterized by the Vosko–Wilk–Nusair (VWN) parameterization [37]. No symmetry restrictions were applied. Ni(II) systems were treated within the unrestricted formalism. The different geometries of the individual chelate systems (starting from either experimental structures (X-ray determined) or pre-optimized by molecular mechanics) were optimized until the maximum and root-mean-squared changes in geometry were below 0.01 and 0.007 Å, respectively. An all electron Triple-ζ Slater-type orbitals (STO) plus one polarization function (TZP) basis set were used for all atoms from the ADF library except for nickel where we applied Ni.2p from TZ2P + basis set. The inner shells were represented by frozen core approximation (1s for C, N, O, and 1s-2p for Ni were kept frozen). Condensed phase effects were treated using a COSMO solvation field (vide infra) as the obtained geometries are far more realistic than those from in vacuo optimization. To obtain single point outputs of the most stable isomer needed for NBO calculation, we employed Gaussian 09 A01 program [38]. For these calculations, we used the unrestricted formalism with B3LYP hybrid functional and the Ahlrichs TZVP basis set [39].

NBO [40] localizes few-center orbitals (“few” meaning typically 1 or 2, but occasionally more) that describe the Lewis-like molecular bonding pattern of electron pairs (or of individual electrons in the open-shell case) in optimally compact form. More precisely, NBOs are an orthonormal set of localized “maximum occupancy” orbitals whose leading $N/2$ members (or N members in the open-shell case) give the most accurate possible Lewis-like description of the total N-electron density.

3. Results and discussion

The pale blue *trans*(O_5)-Mg[Ni(1,3-pd3ap)]·10H_2O and deep blue [Ni(H_2O)$_6$][Ni(1,3-pdta)]·2H_2O have been prepared by reaction of nickel salt with neutralized edta-type acids. X-ray data are reported for [Ni(H_2O)$_6$]·[Ni(1,3-pdta)]·2H_2O. The 1,3-pd3ap with hexadentate coordination can yield two geometrical isomers: the *trans*(O_5) and *trans*(O_5O_6), but only less-strained *trans*(O_5) isomer was observed. The *trans*(O_5) geometry was predicted for $[Ni(pd3ap)]^{2-}$ by interpreting IR and UV/Vis spectroscopy and DFT quantum-mechanical results.

The IR (carboxylate region) and electronic absorption spectra (used for the assignments of complexes) are compared to those of other $[Ni(edta\text{-}type)]^{2-}$ complexes of known structures. The nickel(II)-nickel(II) complex with 1,3-pdta has been synthesized to find possible influence of a transition-metal cation. NBO outputs were used to do more in-depth electronic nickel-edta-type analysis.

3.1. *Description of the crystal structure of [Ni(H_2O)$_6$][Ni(1,3-pdta)]·2H_2O (2)*

An ORTEP drawing of $[Ni(1,3\text{-}pdta)]^{2-}$ and the packing of the molecules are depicted in figure 2; selected bond lengths and angles are listed in table 2. Values for Ni-L bond distances and angles in $[Ni(1,3\text{-}pdta)]^{2-}$ are compared with those obtained for a similar complex [7]. Each asymmetric unit, in our case, contains a half formula unit consisting of a half cationic hydrated Ni-complex, a half anionic Ni-(1,3-propanediaminetetraacetate) complex, and two half waters. The positions of N1, N2, and C6 (2..) and O8 and O9 (..2) of water are all placed at special positions, meaning all moieties have a crystallographically imposed twofold axis. The orthorhombic unit cell contains 16 units, four cations, four anions, and eight waters (figure 2). The *cis* angles at Ni(II) (table 2) range from 82.47(4)° to 97.99(3)°, while the *trans* ones are 175.40(3)° and 173.36(4)°. The six-membered dia-

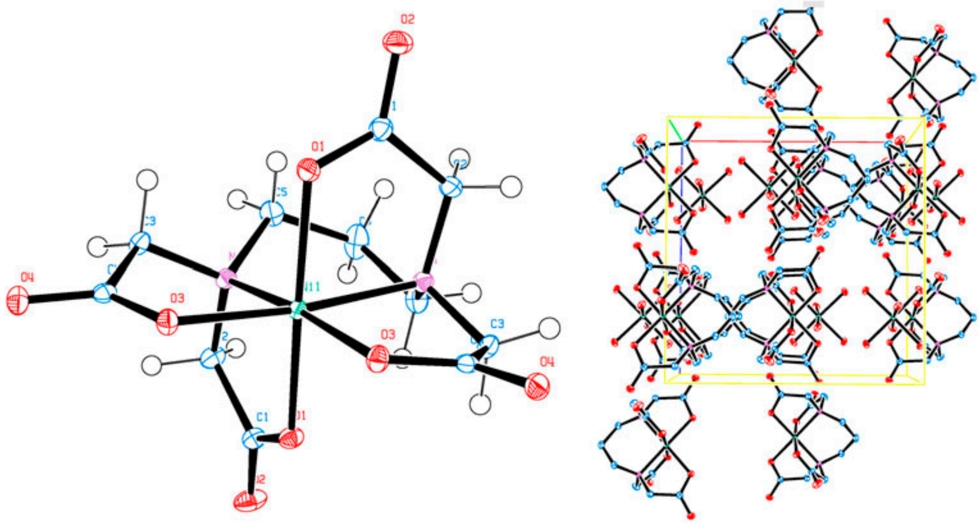

Figure 2. Molecular structure (ORTEP view) of $[Ni(1,3\text{-}pdta)]^{2-}$ (**2**) and the crystal packing view along the *c* axis.

Table 2. Bond distances (Å) and angles (°) with e.s.d.'s in parentheses for [Ni(H_2O)$_6$][Ni(1,3-pdta)]·2H_2O and comparison with *trans*(O_5)-[Ni_2(1,3-pddadp)(H_2O)$_4$]·4H_2O [7].

[Ni(H_2O)$_6$][Ni(1,3-pdta)]·2H_2O				*trans*(O_5)-[Ni_2(1,3-pddadp)(H_2O)$_4$]·4H_2O [7]			
M–L Bond lengths (Å)							
Ni1–O1	2.0807(8)			Ni(1)–O(1)	2.089(2)		
Ni1–O3	2.0277(8)			Ni(1)–O(3)	2.074(3)		
Ni1–O1_a	2.0807(8)			Ni(1)–O(5)	2.060(3)		
Ni1–O3_a	2.0277(8)			Ni(1)–O(7)	2.060(3)		
Ni1–N1	2.0795(10)			Ni(1)–N(1)	2.090(3)		
Ni1–N1_a	2.0795(10)			Ni(1)–N(2)	2.109(3)		
Bond angles (°)							
Cis angles		*Trans* angles		*Cis* angles		*Trans* angles	
O1–Ni1–O3	92.08(3)	O1–Ni1–O1_a	175.40(3)	N(1)–Ni(1)–N(2)	95.7(1)	O(5)–Ni(1)–O(7)	179.3(1)
O1–Ni1–N1	82.47(4)	O3–Ni1–N1_a	173.36(4)	O(7)–Ni(1)–N(2)	81.7(1)	O(3)–Ni(1)–N(1)	168.2(1)
O1–Ni1–O3_a	90.94(3)	N1–Ni1–O3_a	173.36(4)	O(7)–Ni(1)–N(1)	98.1(1)	O(1)–Ni(1)–N(2)	169.1(1)
O1–Ni1–N1_a	94.44(4)			O(5)–Ni(1)–N(2)	97.7(1)		
O3–Ni1–N1	83.17(3)			O(5)–Ni(1)–N(1)	81.7(1)		
O3–Ni1–O1_a	90.94(3)			O(3)–Ni(1)–N(2)	93.4(1)		
O3–Ni1–O3_a	97.99(3)			O(3)–Ni(1)–O(7)	90.6(1)		
N1–Ni1–O1_a	94.44(4)			O(3)–Ni(1)–O(5)	89.7(1)		
N1–Ni1–N1_a	96.44(4)			O(1)–Ni(1)–N(1)	93.6(1)		
O1_a–Ni1–O3_a	92.08(3)			O(1)–Ni(1)–O(7)	91.3(1)		
O1_a–Ni1–N1_a	82.47(4)			O(1)–Ni(1)–O(5)	89.3(1)		
O3_a–Ni1–N1_a	83.17(3)			O(1)–Ni(1)–O(3)	78.2(1)		

mine (T) ring adopts a *skew-boat* conformation. The R rings are almost planar (in an *envelope* conformation), while the G rings are much more puckered and are halfway between *envelope* and *twist* conformations.

A search of the distances yielded intermolecular and intramolecular contacts shorter than the sum of the van der Waals radii [41]; the moieties are linked by hydrogen bonds forming infinite 1-D chains along the base vectors [0 1 0] (see Supplementary material). There are no short contacts between nickel(II) and [Ni(1,3-pdta)]$^{2-}$, usually found in M(II)(EDTA-type)M′(II) complexes [14].

3.2. *Structural parameters and strain analysis*

Some structural parameters (the mean M–L bond lengths and some bond angles) in Ni(1,3-pdta)]$^{2-}$ are given in table 2. For this complex, the mean M-O(G) distances are slightly shorter than the mean M-O(R) distances, not usual for this type of complex. However, the mean M-O(G) distances are shorter than the mean M-N distances, but M-O(R) distances are longer.

Since the DFT calculated geometry of *trans*(O_5)-[Ni(1,3-pd3ap]$^{2-}$ does not deviate significantly from other similar structures, we do not expect the strain analysis to reveal any unusual results. Structural data correlating the stereochemistry of nickel complexes with edta-type ligands are given in table 3. Figure 3 shows the DFT optimized structure of *trans*(O_5)-[Ni(1,3-pd3ap)]$^{2-}$.

The sum of the bite-angle deviations, $\Sigma\Delta(O_h)$, varies from 56° in *trans*(O_5)-Mg[Ni(1,3-pd3ap)]·10H_2O to 74° in [Mg(H_2O)$_6$]·[Ni(1,4-bdta)]·3H_2O, the latter having the greatest distortion of the complexes in table 2. The sum of 58° for [Ni(H_2O)$_6$]·[Ni(1,3-pdta)]·2H_2O and 56° for *trans*(O_5)-Ba[Ni(1,3-pd3ap)]·6H_2O show great distortions. The conformation of the

Table 3. Strain analysis of nickel complexes with edta-type ligands with five- and/or six-membered carboxylate rings.

		$\Delta\Sigma$(ring)[b]			Δ (Ni–O–C)[c]			
Complex	$\Sigma\Delta(O_h)$[a]	E, T or B	R	G	R	G	$\Sigma\Delta$(N)[d]	Ref.
Ni[Ni(1,3-pdta)]·8H_2O	58	+30	+1	−10	+6	+4	11	This work
[Ni_2(1,3-pddadp)$(H_2O)_4$]·4H_2O	60	+28	0	+36	+7	+20	8	[7]
Mg[Ni(1,3-pd3ap)]·10H_2O[e]	56	+31	0	−14(+37)	+7	+5(+19)	15(10)	This work DFT calcd
Mg[Ni(1,3-pndta)]·10H_2O	57	+31	+1	−9	+6	+3	15	[21]
Mg[Ni(1,4-bdta)]·9H_2O	74	+70	−2	−13	+6	+5	23	[20]

[a] $\Sigma\Delta(O_h)$ is the sum of the absolute values of the deviations from 90° of the 12 L–Ni–L' angles. All values rounded off to the nearest degree.

[b] $\Delta\Sigma$(ring) is the deviation from the ideal of the corresponding chelate rings' bond angle sum. Ideal values: 528 and 637.5° for the five- and six-membered diamine ring, respectively, and 538.5° and 648.0° for the five- and six-membered carboxylate ring, respectively.

[c] Δ(Ni–O–C) (ring) is the mean value of the deviation of the corresponding rings' Ni–O–C bond angle from the 109.5°.

[d] $\Sigma\Delta$(N) is the sum of the absolute values of the deviations from 109.5° of the six bond angles made by nitrogen atoms. A mean value for the two nitrogens is reported.

[e] For this complex, having C_1 molecular symmetry, the two values are reported. The values in parentheses are given for the *β*-alaninate rings and nitrogen atoms connecting 3-alaninate rings.

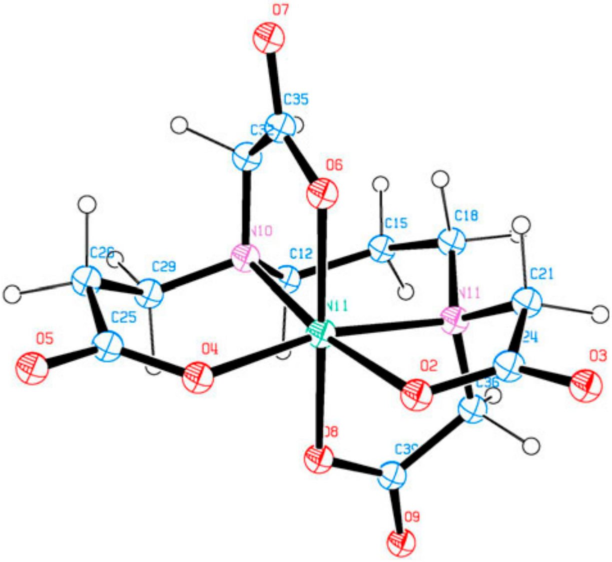

Figure 3. DFT (ADF) optimized structure of *trans*(O_5)-[Ni(1,3-pd3ap)]$^{2-}$.

1,3-propanediamine (T) ring of both complexes is a *skew-boat*. The 1,3-propanediamine ring (T ring) in *trans*(O_5)-[Ni(1,3-pd3ap)]$^{2-}$ shows a positive total deviation of +31°. The same ring in [Ni$(H_2O)_6$]·[Ni(1,3-pdta)]·2H_2O shows total positive deviation of +30°.

Five-membered rings coordinated in the equatorial plane have negative deviations from the ideal chelate ring bond angle sum: −14° in *trans*(O_5)-[Ni(1,3-pd3ap)]$^{2-}$ and −10° in [Ni$(H_2O)_6$]·[Ni(1,3-pdta)]·2H_2O. Contrary to this, five-membered rings coordinated in axial positions show very small positive deviation (+1°) in $[Ni(H_2O)_6]\cdot[Ni(1,3\text{-pdta})]\cdot 2H_2O$, while in *trans*($O_5$)-$[Ni(1,3\text{-pd3ap})]^{2-}$ there is no deviation. Six-membered β-alaninato rings coordinated in the equatorial plane in *trans*(O_5)-$[Ni(1,3\text{-pd3ap})]^{2-}$ have positive deviation (+37°). All complexes show positive deviation of the Ni-O-C(R, G) bond angles. These deviations are less for glycinato rings (from +6° to +7° and from +3° to +5° for the R and G rings, respectively), than for β-alaninato rings (+19° and +20° for the G rings). When each of the deviations for the six angles made by the nitrogens is summed, the total deviations (absolute values) for each complex were obtained. Total deviation about the chelating N sums to roughly 11° for $[Ni(H_2O)_6]\cdot[Ni(1,3\text{-pdta})]\cdot 2H_2O$ and 15°(10°) for *trans*(O_5)-$[Ni(1,3\text{-pd3ap})]^{2-}$. The equatorially coordinated five-membered glycinato rings are more strained than those coordinated axially. Thus, it appears that equatorial orientation of β-alaninato ring has no influence on the strain of these systems, also found in Ni-1,3-pddadp, favoring *trans*(O_5) geometry in both 1,3-pddadp and 1,3-pd3ap. Similar strain has been found in $Mg[Ni(1,3\text{-pndta})]\cdot 10H_2O$ [21] while much more deviation ($\Sigma\Delta(O_h) = 74°$ and $T = +70$) was observed for $Mg[Ni(1,4\text{-bdta})]\cdot 9H_2O$ [20].

3.3. *Spectral analysis*

Asymmetric stretching vibrations for Ni-edta-type complexes are given in table 4. The asymmetric stretching carboxylate frequencies have been established as criteria for distinguishing between protonated carboxylate (1700–1750 cm^{-1}) and coordinated carboxylate (1600–1650 cm^{-1}) [42–44]. The complexes show absorptions in agreement with their molecular symmetries (C_1 for *trans*(O_5)-$Mg[Ni(1,3\text{-pd3ap})]\cdot 10H_2O$ and C_2 for $[Ni(H_2O)_6]\cdot[Ni(1,3\text{-pdta})]\cdot 2H_2O$). For *trans*($O_5$)-$[Ni(1,3\text{-pd3ap})]^{2-}$ of C_1 symmetry, the IR spectrum contains one strong broad band centered at 1595 cm^{-1}. Normally, two bands are expected due to the asymmetric vibrations of five-membered glycinato rings and six-membered β-alaninate rings. However, due to mixing with lattice water vibrations, we do not observe all distinct vibrations. For $[Ni(H_2O)_6]\cdot[Ni(1,3\text{-pdta})]\cdot 2H_2O$ of C_2 symmetry, the IR spectrum contains one strong broad band at 1587 cm^{-1}. The lack of other absorptions in the 1700–1750 cm^{-1} range suggests that all the carboxylates are coordinated.

Ligand field absorption spectra for $[Ni(H_2O)_6]\cdot[Ni(1,3\text{-pdta})]\cdot 2H_2O$ and *trans*(O_5)-$Mg[Ni(1,3\text{-pd3ap})]\cdot 10H_2O$ and related edta-type complexes are given in figure 4 (table 5). All complexes forming six-membered diamine (T) rings, compared to those of related complexes forming five-membered diamine (E) rings, show broadening of the first absorption band (lower energy side, figure 4) due to the influence of tetragonality on the spectro-

Table 4. Asymmetric carboxylate stretching frequencies for $[Ni(\text{edta-type})]^-$ complexes[a].

Complex	ν_{asym} (COOM)	Chelate ring size	Ref.
$[Ni(H_2O)_6]\cdot[Ni(1,3\text{-pdta})]\cdot 2H_2O$	1587	5	This work
trans(O_5)-$[Ni_2(1,3\text{-pddadp})(H_2O)_4]\cdot 4H_2O$	1640sh	5	[7]
	1591	6	
trans(O_5O_6)-$Na_2[Ni(1,3\text{-pddadp})]\cdot 3H_2O$	1635sh	5	[7]
	1610		
	1588	6	
trans(O_5)-$Mg[Ni(1,3\text{-pd3ap})]\cdot 10H_2O$	1595	5 and 6	This work
$Mg[Ni(1,3\text{-pndta})]\cdot 10H_2O$	1597	5	[21]

[a]Values are given in cm^{-1}.

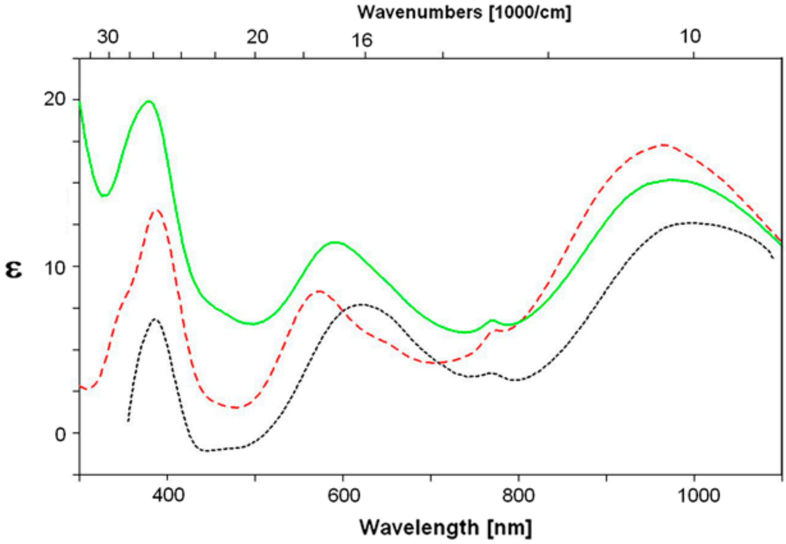

Figure 4. Electronic absorption spectra of Ni(II) complexes: - - - - pdta; ▬ pd3ap; ------ pddadp.

Table 5. Absorption data for some [Ni(edta-type)]) complexes[a].

Complex		10^3 ν(cm^{-1})	ε	Assignments O_h	Ref.
Mg[Ni(1,3-pdta)]·8H_2O	I	10.50	16.6	$^3A_{2g}$ → $^3T_{2g}(F)$	[18]
	II	12.98	3.9	→ $^1E_g(D)$	
	III	17.54	6.8	→ $^3T_{1g}(F)$	
	IV	26.37–28.57sh	7.6	→ $^3T_{1g}(P)$	
[Ni(H_2O)$_6$]·[Ni(1,3-pdta)]·2H_2O	I	10.35	17.31		This work
	II	12.87	6.18		
	III	17.48	8.51		
	IV	25.77	13.43		
trans(O_5)-Mg[Ni(1,3-pd3ap)]·10H_2O	I	10.22	15.2		This work
	II	12.99	6.8		
	III	16.86	11.5		
	IV	26.39	19.9		
trans(O_5)-[Ni_2(1,3-pddadp)(H_2O)$_4$]·4H_2O	I	10.18	11.3		[7]
	II	13.00	2.3		
	III	16.55	6.5		
	IV	26.88	10.0		
Mg[Ni(1,3-pndta)]·10H_2O	I	10.59	14.7		[21]
	II	12.88	4.0		
	III	17.52	6.8		
	IV	26.69sh	7.3		
Mg[Ni(1,4-bdta)]·9H_2O	I	9.63	11.7		[20]
	II	12.97	3.5		
	III	17.21	9.9		
	IV	25.73sh	11.9		

[a] Values ε are given in units of mol^{-1} dm^3 cm^{-1}.

chemical behavior of these complexes (D_{4h} model). However, electronic absorption spectra, as established for Ni(II)-edta-type and most other Ni(II) complexes, can best be interpreted by using an octahedral model (O_h): ${}^3A_{2g}\rightarrow{}^3T_{2g}(F)$ (band I); ${}^3A_{2g}\rightarrow{}^3T_{1g}(F)$ (band III), and ${}^3A_{2g}\rightarrow{}^3T_{1g}(P)$ (band IV) (table 5). As expected, the aqueous spectra of $[Ni(H_2O)_6]\cdot[Ni(1,3\text{-pdta})]\cdot 2H_2O$ and *trans*(O_5)-Mg[Ni(1,3-pd3ap)]$\cdot 10H_2O$ show a shoulder at 13,000 cm^{-1} which occurs on the high-energy side of the first spin-allowed band (band II, table 5). This band probably arises from a spin-forbidden triplet to singlet transition. The absorption maxima of $[Ni(H_2O)_6]\cdot[Ni(1,3\text{-pdta})]\cdot 2H_2O$ and *trans*(O_5)-Mg[Ni(1,3-pd3ap)]$\cdot 10H_2O$ (bands I and III, table 5) are located at lower energies than those found for Mg[Ni(1,3-pdta)]$\cdot 8H_2O$ [18]. The ligand field strength (LFS) for these complexes increases in the order pddadp < pd3ap < pdta with the decreasing number of six-membered rings in the G plane.

3.4. *DFT calculations*

ADF is a Fortran program for calculations on atoms and molecules. It can be used for Ni(II) complexes. We optimized geometries of each of the potential geometric isomers, except *trans*(O_6)-[Ni(1,3-pddadp)]. For the search global minima, we have chosen Perdew–Wang (PW91) [36] correlation gradient corrections as this proved to be the best choice in our case. table 6 contains structural parameters correlating ADF and experimental data (where we have it) of edta-type of nickel(II) complexes. First, we preoptimized a particular isomer by molecular mechanics MM+ and then left the structures to be optimized by ADF2007.01. In cases where we had crystal structures, we used them directly for optimization. Since nickel has two unpaired electrons and triplet multiplicity, the systems were treated within the unrestricted formalism. We decided to compare energies, bond lengths Ni-N in plane, Ni-O in plane, Ni-O axial and average

Table 6. Comparison of experimental and DFT (ADF) data for edta-type nickel(II) complexes.

Ligand	$[Ni(1,3\text{-pdta})]^{2-}$	$[Ni(1,3\text{-pddadp})]^{2-}$		$[Ni(1,3\text{-pd3ap})]^{2-}$	
Reference	This work	[7]		This work	
Geometrical isomer[a]	No isomers	*Trans*(O_5O_6)	0	*Trans*(O_5)	0
		Trans(O_5)	0.5	*Trans*(O_5O_6)	4.45
		Trans(O_6)	386		
Comparison of experimental (X-ray) and lowest energy DFT-optimized structure					
Ni-N (Å) in-plane	2.079:2.112	2.090:2.148		:2.145	
Exp: DFT	2.079:2.112	2.109:2.145		:2.138	
Ni-O (Å) in-plane	2.028:2.085	2.089:2.107		:2.105	
Exp: DFT	2.028:2.085	2.074:2.097		:2.055	
Ni-O (Å) axial	2.081:2.087	2.060:2.082		:2.087	
Exp: DFT	2.081:2.087	2.060:2.078		:2.080	
Ni–O–C (o) (av.)	114.6:113.9	123.13:123.5		:118.7	
Exp: DFT					
Ni–O–C–O (o) (av.)	173.94:177.7	168.3:169.7		:174.3	
Exp: DFT					
cis-angles (°) (av.)	90.1:90.0	90.1:90.1		:90.1	
Exp: DFT					
trans-angles (°) (av.)	174.0:175.4	172.2:172.5		:171.3	
Exp: DFT					

[a] The isomer with the lowest energy minimum has been indicated with 0 kcal mol^{-1}.

of Ni–O–C and Ni–O–C–O, *cis*- and *trans*-angles. For all complexes where we have structural data, the ADF theory gave the lowest energy isomer (table 6). In the case of $[Ni(1,3\text{-pd3ap})]^{2-}$ DFT theory shows that *trans*(O_5) isomer is more stable by 4.45 $kcal\,mol^{-1}$ than *trans*(O_5O_6) (table 6). All bonds are sometimes significantly and sometimes slightly longer than ones found in crystal structures. This might be attributed to DFT calculations on molecules in solid state but also to the choice of exchange and correlation gradient potentials.

3.5. *NBO analysis*

Complex anion is fragmented in two separated units, Ni(II) and edta-type^{4-}. The energies from donor–acceptor (D–A) mechanism have been obtained by analyzing quantum-mechanical output files calculated by GENNBO EES. In case of nickel complexes, fragmentation on two sub-units is pronounced with all nickel chelates of edta-type ligands used. Here, we describe NBO results mainly within Ni^{2+} and 1,3-pd3ap^{4-} units. However, similar relations were found for Ni-1,3-pdta and Ni-1,3-pddadp. The most intensive D–A energy transfers in the equatorial plane are result of donation of electronic charge, from lone "*p*" electron pairs of carboxylate oxygens as well as from sp^n tetrahedral nitrogens, toward virtual "non-Lewis" $LP(D_{x2\text{-}y2})^*$ orbital of nickel. The "LP*" label denotes a 1c (lone) non-Lewis (*) orbital of the formal valence shell (hence, distinguished from Rydberg-type "RY*"). It occurs primarily in formally hypovalent species, such as the empty p-type valence orbital of B in boranes or the empty s- or d-type valence orbitals of Ni in our example [40]. The most intensive donor-acceptor energy transfers in an axial plane result from donation of electronic charge, from lone "*p*" electron pairs of carboxylate oxygens toward "non-Lewis" $LP(D_{z2})^*$ orbital of nickel.

The structure of *trans*(O_5)-$[Ni(1,3\text{-pd3ap})]^{2-}$ is given in figure 5, involving donor-acceptor mechanism of PNBO (preorthogonal-natural-bond-orbitals). Comparison of D–A

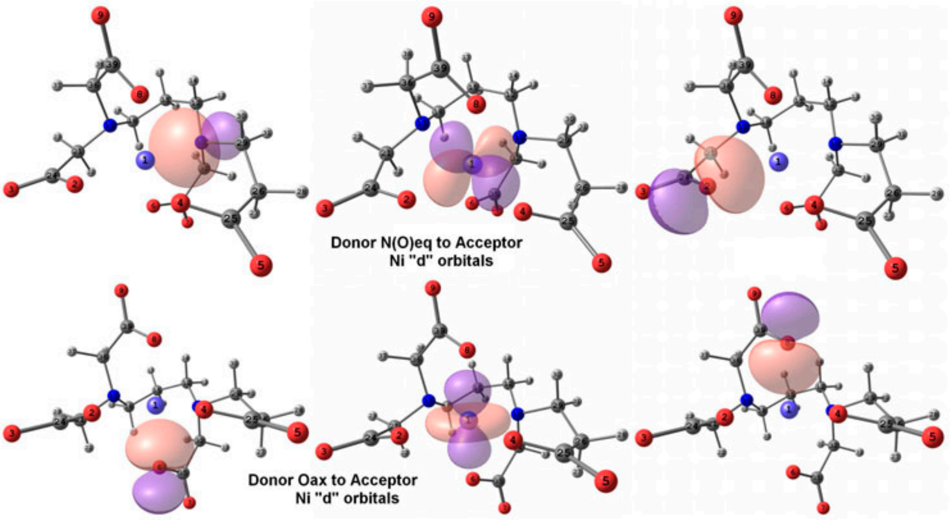

Figure 5. Donor–acceptor PNBO scheme of *trans*(O_5)-$[Ni(1,3\text{-pd3ap})]^{2-}$ from the D–A mechanism.

Table 7. Energies from donor-acceptor (NBO) interactions (kcal/mol).

	Complexes		
	$[Ni(1,3\text{-pdta})]^{2-}$	$[Ni(1,3\text{-pd3ap})]^{2-}$	$[Ni(1,3\text{-pddadp})]^{2-}$
α-DA energy	98.82	103.14	98.81
β-DA energy	184.26	182.07	174.16
Total energy	283.08	285.21	272.97

energies is given in table 7. Generally, the DA charges are mainly affected by β transfers. Accordingly the more six-membered rings in the equatorial plane the lower the DA interactions. $[Ni(1,3\text{-pd3ap})]^{2-}$ gives four strongly interacting hyperbond carboxylate O-:C:O resonance triads, as expected. Other three center (3C:) hyperbonds have not been found in this complex anion.

4. Conclusions

We report preparation, chromatography, and characterization of hexadentate $Mg[Ni(1,3\text{-pd3ap})]\cdot 10H_2O$ containing unsymmetrical edta-type 1,3-pd3ap^{2-}. Only [*trans*(O_5)] of the two possible geometrical isomers was isolated. In this isomer, the two five-membered glycinate rings (R rings) occupy *trans*-axial sites while one glycinate and one β-alaninate ring lie in the equatorial plane along with two nitrogens (G rings). To observe the cation influence on the structural and electronic behavior, $[Ni(H_2O)_6][Ni(1,3\text{-pdta})]\cdot 2H_2O$ was prepared and its structure verified by X-ray analysis. We did not observe short contacts between nickel(II) and $[Ni(1,3\text{-pdta})]^{2-}$, usually found in M(II)(EDTA-type)M′(II) complexes [14]. The structural assignment was made on the basis of DFT, IR, and UV–Vis spectral data. IR and UV–Vis data indicate octahedral coordination around nickel with all carboxylates deprotonated and coordinated. DFT–NBO analysis suggests that within nickel (II) complexes there are two distinct ionic units nickel(II) cation and edta-type tetraanion. The units exhibit a strong donor-acceptor mechanism. According to UV–Vis spectral results of our complexes and several with similar structures, the LFS increases in the order pddadp < pd3ap < pdta with decreasing number of six-membered rings in the G plane.

Supplementary material

Crystallographic details of the complex in the form of CIF files are available and have the CCDC number 900017. These data can be obtained free of charge from the Cambridge Crystallographic Data Center, 12 Union Road, Cambridge CB2 1EZ, UK; Fax: þ44 1223336033 or Email: deposit@ccdc.cam.ac.uk.

Acknowledgement

The authors are grateful to the Serbian Ministry for Education, Science and Technology for financial support (Project No. 41010).

References

[1] T. Kowalik-Jankowska, H. Kozlowski, E. Farkas, I. Sovago. In *Nickel and Its Surprising Impact in Nature*, A. Sigel, H. Sigel, R.K.O. Sigel (Eds), Vol. 2, pp. 31–109, Wiley, New York (2007) and references therein.
[2] U. Ermler, W. Grabarse, S. Shima, M. Goubeaud, R.K. Thauer. *Curr. Opin. Struct. Biol.*, **8**, 749 (1998).
[3] Agency for Toxic Substances and Disease Registry, ATSDR. *Toxicological profile for nickel*, U.S. Department of Health and Human Services, Public Health Service, Atlanta, GA (2003).
[4] D.J. Radanović. *Coord. Chem. Rev.*, **54**, 159 (1984) and references therein.
[5] B.E. Douglas, D.J. Radanović. *Coord. Chem. Rev.*, **128**, 139 (1993).
[6] D.J. Radanović, S. Ianelli, G. Pelosi, Z.D. Matović, S. Tasić-Stojanović, B.E. Douglas. *Inorg. Chim. Acta*, **278**, 66 (1998) and references therein.
[7] Z.D. Matović, S. Ianelli, G. Pelosi, S.K. Janicijević, V.M. Ristanović, G. Ponticelli, D.J. Radanović. *Polyhedron*, **21**, 2667 (2002).
[8] Z.D. Matović, V.D. Miletić, G. Samardžić, G. Pelosi, S. Ianelli, S. Trifunović. *Inorg. Chim. Acta*, **358**, 3135 (2005).
[9] Z.D. Matović, A. Meetsma, V.D. Miletić, P.J. van Koningsbruggen. *Inorg. Chim. Acta*, **360**, 2420 (2007).
[10] (a) H.A. Weakliem, J.L. Hoard. *J. Am. Chem. Soc.*, **81**, 549 (1959); (b) K. Okamoto, T. Tsukihara, J. Hidaka, Y. Shimura. *Bull. Chem. Soc. Jpn.*, **51**, 3534 (1978).
[11] Y. Kushi, K. Morimasa, H. Yoneda. This is a paper presented at a conference. In *49th Annual Meeting of the Chemical Society of Japan*, Abstract No. 1 N31, Tokyo, April (1984).
[12] (a) N.V. Novozhilova, T.N. Polynova, M.A. Porai-Koshits, N.I. Pechurova, L.I. Martynenko, A. Khadi. *Zh. Strukt. Khim.*, **14**, 745 (1973); (b) Y. Kushi, K. Morimasa, K. Yoshitsugu, H. Yoneda. *35th Symposium Coordination Chemistry*, Abstract 2B01, Hiroshima, Japan (1985).
[13] (a) T. Lis. *Acta Crystallogr., Sect. B*, **B34**, 1342 (1978); (b) J. Stein, J.P. Fackler, Jr., G.J. McClune, J.A. Fee, L.T. Chan. *Inorg. Chem.*, **18**, 3511 (1979).
[14] X. Solans, M. Font-Altaba, J. Oliva, J. Herrera. *Acta Crystallogr., Sect. C*, **C39**, 435 (1983).
[15] (a) E.F.K. McCandlish, T.K. Michael, J.A. Neal, E.C. Lingafelter, N.J. Rose. *Inorg. Chem.*, **17**, 1383 (1978); (b) A.I. Pozhidaev, N.N. Neronova, T.N. Polynova, M.A. Porai-Koshits, V.A. Logvinenko. *Zh. Strukt. Khim.*, **13**, 344 (1972).
[16] E. Coronado, M. Drillon, A. Fuertes, D. Beltran, A. Mosset, J. Galy. *J. Am. Chem. Soc.*, **108**, 900 (1986).
[17] V.D. Miletić, A. Meetsma, P.J. van Koningsbruggen, Z.D. Matović. *Inorg. Chem. Commun.*, **12**, 720 (2009).
[18] D.J. Radanović, T. Ama, H. Kawaguchi, N.S. Drašković, D.M. Ristanović, S. Janićijević. *Bull. Chem. Soc. Jpn.*, **74**, 701 (2001).
[19] S. Domínguez, A. Mederos, P. Gili, A. Rancel, A.E. Rivero, F. Brito, F. Lloret, X. Solans, C. Ruíz-Pérez, M.L. Rodríguez, I. Brito. *Inorg. Chim. Acta*, **255**, 367 (1997).
[20] D.D. Radanović, U. Rychlewska, B. Warzajtis, M.S. Cvijovic, M. Dj. *Dimitrijević, M.I. Djuran. Polyhedron*, **26**, 4799 (2007).
[21] N.S. Drašković, D.D. Radanović, U. Rychlewska, B. Warżajtis, I.M. Stanojević, M.I. Djuran. *Polyhedron*, **43**, 185 (2012).
[22] J.A. Weyh, R.E. Hamm. *Inorg. Chem.*, **7**, 2431 (1968).
[23] Bruker. *SMART, SAINT, SADABS, XPREP and SHELXTL/NT, Area Detector Control and Integration Software, Smart Apex Software Reference Manuals*, Bruker Analytical X-ray Instruments. Inc., Madison, Wisconsin, USA (2000).
[24] G.M. Sheldrick. *SADABS. Version 2*. Multi-Scan Absorption Correction Program, University of Göttingen, Germany (2001).
[25] A.J.M. Duisenberg. *J. Appl. Crystallogr.*, **25**, 92 (1992).
[26] A.L. Spek. *J. Appl. Crystallogr.*, **21**, 578 (1988).
[27] Y. Le Page. *J. Appl. Crystallogr.*, **20**, 264 (1987).
[28] Y. Le Page. *J. Appl. Crystallogr.*, **21**, 983 (1988).
[29] A. Altomare, M.C. Burla, M. Camalli, G.L. Cascarano, C. Giacovazzo, A. Guagliardi, A.G.G. Moliterni, G. Polidori, R. Spagna. *J. Appl. Crystallogr.*, **32**, 115 (1999). SIR-97. *A package for crystal structure solution by direct methods and refinement*, Univ. of Bari, Univ. of Perugia and Univ. of Roma, Italy.
[30] G.M. Sheldrick. *SHELXL-97*, *Program for the Refinement of Crystal Structures*, University of Göttingen, Germany (1997).
[31] A. Meetsma. *PLUTO*, *Molecular Graphics Program (Version of April 2004)*, University of Groningen, The Netherlands (2004).
[32] A.L. Spek. *PLATON, Program for the Automated Analysis of Molecular Geometry (A Multipurpose Crystallographic Tool) (Version of April 2004)*, University of Utrecht, The Netherlands (2004).
[33] ADF2009.01., ADF2007.01. ADF2004.01.SCM, Theoretical chemistry, Vrije Universiteit Amsterdam, The Netherlands. Available online at: http://www.scm.com (accessed May 2012).
[34] C.F. Guerra, J.G. Snijders, G. te Velde, E.J. Baerends. *Theor. Chem. Acc.*, **99**, 391 (1998).
[35] G. te Velde, F.M. Bickelhaupt, S.J.A. van Gisbergen, C.F. Guerra, E.J. Baerends, J.G. Snijders, T. Ziegler. *J. Comput. Chem.*, **22**, 931 (2001).

[36] J.P. Perdew, J.A. Chevary, S.H. Vosko, K.A. Jackson, M.R. Pederson, D.J. Sing, C. Fiolhais. *Phys. Rev. B*, **46**, 6671 (1992).
[37] S. Vosko, L. Wilk, M. Nusair. *Can. J. Phys.*, **58**, 1200 (1980).
[38] M.J. Frisch, G.W. Trucks, H.B. Schlegel, G.E. Scuseria, M.A. Robb, J.R. Cheeseman, G. Scalmani, V. Barone, B. Mennucci, G.A. Petersson, H. Nakatsuji, M. Caricato, X.Li, H.P. Hratchian, A.F. Izmaylov, J. Bloino, G. Zheng, J.L. Sonnenberg, M. Hada, M. Ehara, K. Toyota, R. Fukuda, J. Hasegawa, M. Ishida, T. Nakajima, Y. Honda, O. Kitao, H. Nakai, T. Vreven, J.A. Montgomery, Jr., J.E. Peralta, F. Ogliaro, M. Bearpark, J.J. Heyd, E. Brothers, K.N. Kudin, V.N. Staroverov, R. Kobayashi, J. Normand, K. Raghavachari, A. Rendell, J.C. Burant, S.S. Iyengar, J. Tomasi, M. Cossi, N. Rega, J.M. Millam, M. Klene, J.E. Knox, J.B. Cross, V. Bakken, C. Adamo, J. Jaramillo, R. Gomperts, R.E. Stratmann, O. Yazyev, A.J. Austin, R. Cammi, C. Pomelli, J.W. Ochterski, R.L. Martin, K. Morokuma, V.G. Zakrzewski, G.A. Voth, P. Salvador, J.J. Dannenberg, S. Dapprich, A.D. Daniels, Ö. Farkas, J.B. Foresman, J.V. Ortiz, J. Cioslowski, D.J. Fox. *Gaussian 09 (Revision A.1)*, Gaussian, Inc., Wallingford, CT (2009).
[39] F. Weigend, R. Ahlrichs. *PCCP*, **7**, 3297 (2005).
[40] E.D. Glendening, J.K. Badenhoop, A.E. Reed, J.E.Carpenter, J.A. Bohmann, C.M. Morales, F. Weinhold. *NBO 5.0*, Theoretical Chemistry Institute, University of Wisconsin, Madison (2001).
[41] A. Bondi. *J. Phys. Chem.*, **68**, 441 (1964).
[42] D.H. Busch, J.C. Bailar., Jr. *J. Am. Chem. Soc.*, **75**, 4574 (1953).
[43] M.L. Morris, D.H. Busch. *J. Am. Chem. Soc.*, **78**, 5178 (1956).
[44] K. Nakamoto. *Infrared Spectra of Inorganic and Coordination Compounds*, Wiley, New York, NY (1963).